

PAPER • OPEN ACCESS

Electronic, Raman and vibrational properties of $\text{Ag}_m \text{Cu}_n$ ($m + n = 3-6$) clusters: First principles study

To cite this article: Weiyin Li *et al* 2019 *IOP Conf. Ser.: Mater. Sci. Eng.* **490** 022053

View the [article online](#) for updates and enhancements.

Electronic, Raman and vibrational properties of Ag_mCu_n ($m + n = 3-6$) clusters: First principles study

Weiyan Li^{1,*}, Yongli Zhang¹, Sha Zhang¹, Lian Hai¹, and Wenqiang Ma²

¹Key Laboratory of Physics and Photoelectric Information Functional Materials Sciences and Technology, School of Electrical and Information Engineering, North Minzu University, Yinchuan 750021, China

²School of Physics and Electronic Information and Henan Key Laboratory of Electromagnetic Transformation and Detection, Luoyang Normal University, Luoyang, Henan, China

*Corresponding author e-mail: lwy744019@163.com

Abstract. The electronic, Raman and vibrational properties of Ag_mCu_n ($m + n = 3-6$) nanoclusters were investigated using first principles. Results indicate that the electronegativity, hardness, softness, electrophilicity index, and energy gap vary with copper atom adding. Ag_5Cu_1 cluster has the maximum energy gap and hardness, Ag_1Cu_2 cluster has the maximum electronegativity, Ag_2Cu_1 cluster has the maximum softness and electrophilicity index. Their Raman and vibrational spectra are related with their compositions, sizes, and geometries. As the amount of copper atom adds, the strongest Raman peaks of 3-6-atom silver-copper move large wavelength, and the strongest vibrational peaks of 3-atom, 5-atom (except Ag_2Cu_3), and 6-atom (except Ag_3Cu_3) silver-copper clusters also have a trend to shift large wavenumber. The wavenumber of the maximum vibrational peak of Ag_3Cu_1 is the largest and the wavenumber of the maximum vibrational peak of Ag_2Cu_2 is the smallest among the 4-atom silver-copper clusters.

1. Introduction

Bimetallic clusters have particular optical [1, 2], and magnetic properties, so they are potentially applied in the field of solar cell [3, 4], catalysis [5, 6] and so on. Their physical and chemical properties usually are different from their the bulk and may be mediated by their composition and size and so on [7-9]. The bimetallic noble clusters such as silver-copper are very hot due to their large scale potential applications. However, the relationships between structure and physical and chemical properties of silver-copper clusters are not substantially investigated.

There are some complexities in experimental production of silver-copper cluster and there are wide size and shape distributions, therefore, their characterization become difficult. Generally speaking, the sizes and shapes of most clusters are related to their optical, vibrational and Raman spectra. Conversely, the size and shape of the clusters can be characterized by their optical, vibrational and Raman spectra, and even their structures can be predicted by their optical, vibrational and Raman spectra. Bishea et al. [10, 11] obtained the silver-copper binding energy and vibrational bands of AgCu_2 cluster using resonant two-photon ionisation spectrometry, and they analyzed four band systems in the range of 20,000-27,000 cm^{-1} . Cazayous et al. [12] investigated vibrational types of silver-copper nanoparticles using micro-Raman spectroscopy, they found that the silver-copper and



pure silver nanoparticles have two distinct contributions in the same Raman spectroscopy. James et al. [13] studied adiabatic ionization potential of neutral bimetallic CuAg, and dissociation energy and frequency of cationic CuAg⁺ clusters using photoionization spectroscopy technique. Ranjan et al. [14-16] studied electronic and optical properties of mixed and impurity-doped bimetallic CuAg, AgAu, and CuAu clusters using density functional theory (DFT) methodology. Recently, we systematic calculated the electronic, Raman and vibrational properties of seven, eight and thirteen-atom silver-copper nanoclusters [17-24]. Therefore, there is an important role for vibrational and Raman models of silver-copper clusters using the theoretical prediction. Some studies have concentrated on structural and absorption spectra of pure silver and copper nanoclusters, but the systematic investigations on electronic properties, vibrational and Raman spectra of silver-copper nanoclusters are extremely limited till date.

Consequently, this paper systematically study on electronic properties, Raman and vibrational spectra of Ag_mCu_n ($m + n = 3-6$) clusters by means of DFT. Their Raman and vibrational spectra would be conducive to confirming the sizes, structures, and compositions of these nanoclusters.

2. Computing methods

The structures of silver-copper clusters were displayed in the Ref. [25]. During DFT calculations, the exchange-correlation functional is Perdew–Burke–Ernzerhof (PBE) [26]. A global cutoff of grid integration is 5.5 Å. The wavelength of incident light for Raman spectra were simulated at 514.5 nm and 10 K. All computations used Dmol³ package [27, 28].

According to Koopmans' approximation [29], electron affinity (*EA*) and ionization energy (*IE*) of all the nanoalloys are as following:

$$EA = -\varepsilon_{\text{LUMO}} \quad (1)$$

$$IE = -\varepsilon_{\text{HOMO}} \quad (2)$$

where, HOMO is the highest occupied molecular orbital energy of nanoalloys, LUMO is the lowest unoccupied molecular orbital of nanoalloys.

The energy gap (E_{gap}) between HOMO and LUMO is as following:

$$E_{\text{gap}} = \text{LUMO} - \text{HOMO} \quad (3)$$

Therefore, the electronegativity (χ), molecular softness (*S*), global hardness (η), and electrophilicity index (ω) were computed using *I* and *A*. The equations are as following:

$$\chi = -\mu = (IE + EA)/2 \quad (4)$$

$$\eta = (IE - EA)/2 \quad (5)$$

$$S = 1/2\eta \quad (6)$$

$$\omega = \mu^2 S \quad (7)$$

where, μ is the chemical potential of the nanoalloys.

3. Results and discussions

The calculated electronegativity, molecular softness, global hardness, and electrophilicity index on the basis of electronic structure theory, and energy gap of 3-6-atom silver-copper clusters are given in Figure 1. For 3-atom silver-copper clusters, when the amount of copper atom increases, E_{gap} and hardness values increase; electrophilicity index values decrease; electronegativity values fluctuate; the softness of the 3-atom cluster reaches its maximum when the composition of the cluster is Ag₂Cu₁ cluster. For the 4- and 5-atom silver-copper clusters, the E_{gap} , η and χ values increase, while *S* and ω values reduce when the amount of copper atom adds. For the 6-atom silver-copper nanoclusters, with the amount of copper atom increasing, E_{gap} and η values firstly decrease, then increase; χ values firstly decrease, then increase, and then decrease; *S* and ω values have maximum values at the compositions of Ag₂Cu₄ and Ag₃Cu₃ cluster, respectively.

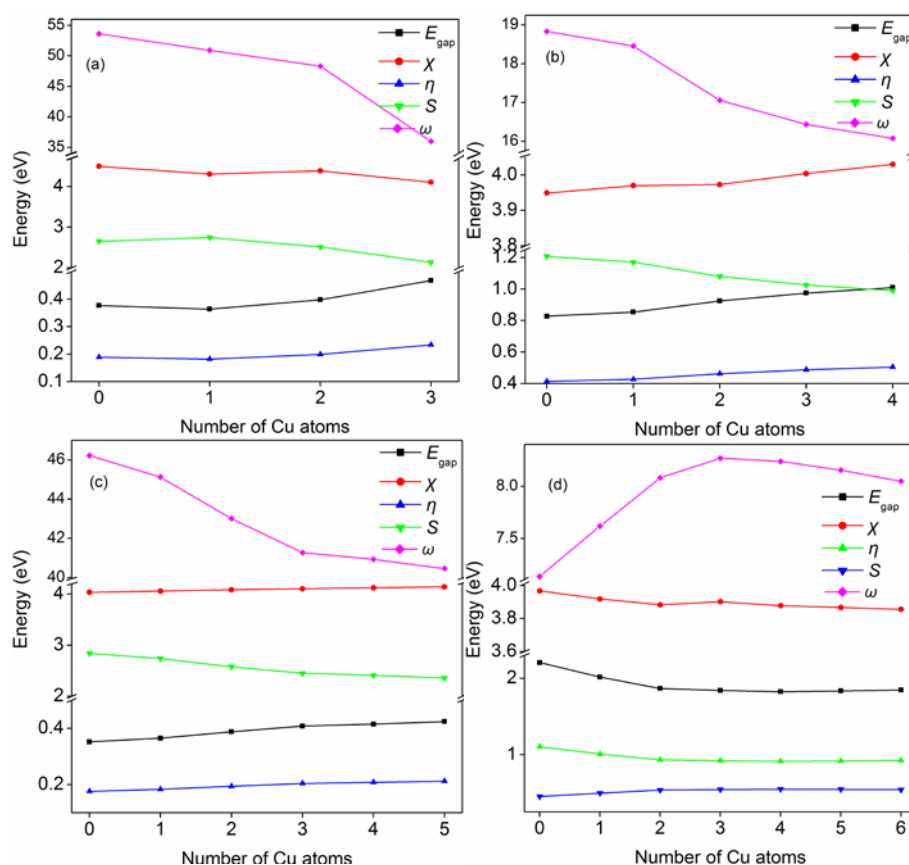


Figure 1. The energy gap, electronegativity, global hardness, molecular softness, and electrophilicity index of 3-6-atom silver-copper clusters.

Figure 2 exhibits Raman and vibrational spectra for 3-atom silver-copper nanoclusters. The Raman spectra of Ag_2Cu_1 and Ag_1Cu_2 show three peaks. The wavelengths of the most intense peaks of Ag_2Cu_1 and Ag_1Cu_2 clusters are smaller than those of the pure Ag_3 and Cu_3 . The intensities of the strongest peaks of Ag_2Cu_1 and Ag_1Cu_2 are weaker than that of Ag_3 cluster, but are stronger than that of the Cu_3 cluster. There is a shift in the Raman spectra and a decrease in the main peak intensity when cluster composition changes from Ag_2Cu_1 to Ag_1Cu_2 . and (Figure 2a-d). The vibrational spectra of Ag_2Cu_1 and Ag_1Cu_2 also show three peaks. The hybrid clusters show larger wavenumbers compare to pure Ag_3 cluster, while the strongest peak wavenumber of pure Cu_3 cluster is located between the Ag_2Cu_1 and Ag_1Cu_2 clusters. As the amount of copper atom increases, the intensities of the strongest vibrational peaks become strong. The wavenumber of Ag_2Cu_1 is smaller than that of Ag_1Cu_2 cluster (Figure 2e-h).

Figure 3 shows the Raman and vibrational spectra of 4-atom silver-copper nanoclusters. There are three peaks in Raman spectrum of Ag_3Cu_1 cluster and two peaks in the spectra of Ag_2Cu_2 and Ag_1Cu_3 clusters. As the amount of copper atom adds, the wavelengths of the strongest peaks become larger, the intensities of the strongest peaks become weaker (Figure 3a-e). The vibrational spectra of Ag_3Cu_1 , Ag_2Cu_2 and Ag_1Cu_3 clusters show four, two and three peaks, respectively (Figure 3g-i). The wavenumber of the strongest peak of Ag_3Cu_1 cluster is the largest among the three silver-copper clusters, however, its peak intensity is the weakest (Figure 3g). The wavenumber of the strongest peak of Ag_2Cu_2 is less than Ag_1Cu_3 and Cu_4 , while its intensity is the strongest (Figure 3h). The wavenumber of the strongest peak of Ag_1Cu_3 is bigger than Ag_2Cu_2 but is less than Cu_4 (Figure 3i).

Figure 4 shows the Raman and vibrational spectra of 5-atom silver-copper clusters, their Raman and vibrational spectra become complicated and have many peaks. For their Raman spectra, wavelengths of the strongest peaks of four silver-copper nanoclusters are bigger than Ag_5 and less than Cu_5 , however, their intensities are weaker than Ag_5 and stronger than Cu_5 (Figure 4a-f). Among their Raman spectra, Ag_1Cu_4 has the largest wavelength, Ag_4Cu_1 has the smallest wavelength,

Ag_2Cu_3 has the strongest intensity, Ag_1Cu_4 has the weakest intensity (Figure 4b-e). For the strongest peaks of vibrational spectra of 5-atom silver-copper nanoclusters, their wavenumbers are larger than Ag_5 and smaller than Cu_5 , the intensity of Ag_5 is stronger than Ag_1Cu_4 , Ag_2Cu_3 and Ag_3Cu_2 and is weaker than Ag_4Cu_1 , the intensity of Cu_5 is stronger than Ag_1Cu_4 and Ag_2Cu_3 and is weaker than Ag_4Cu_1 and Ag_3Cu_2 (Figure 4g-l). For the strongest peak of vibrational spectra of four silver-copper nanoclusters, Ag_1Cu_4 has the largest wavenumber, Ag_4Cu_1 has the smallest wavenumber, the wavenumber of Ag_2Cu_3 is slightly larger than Ag_3Cu_2 , Ag_4Cu_1 has the strongest intensity, Ag_2Cu_3 has the weakest intensity, the intensity of Ag_3Cu_2 is stronger than Ag_1Cu_4 (Figure 4h-k).

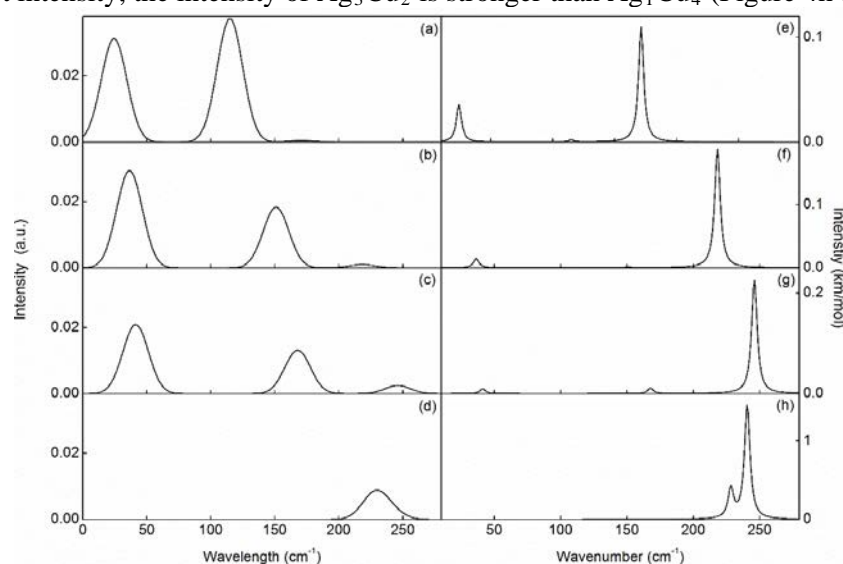


Figure 2. Raman and vibrational spectra of Ag_3 (a, e), Ag_2Cu_1 (b, f), Ag_1Cu_2 (c, g) and Cu_3 (d, h) clusters. Left row is Raman spectrum, right row is vibrational spectrum.

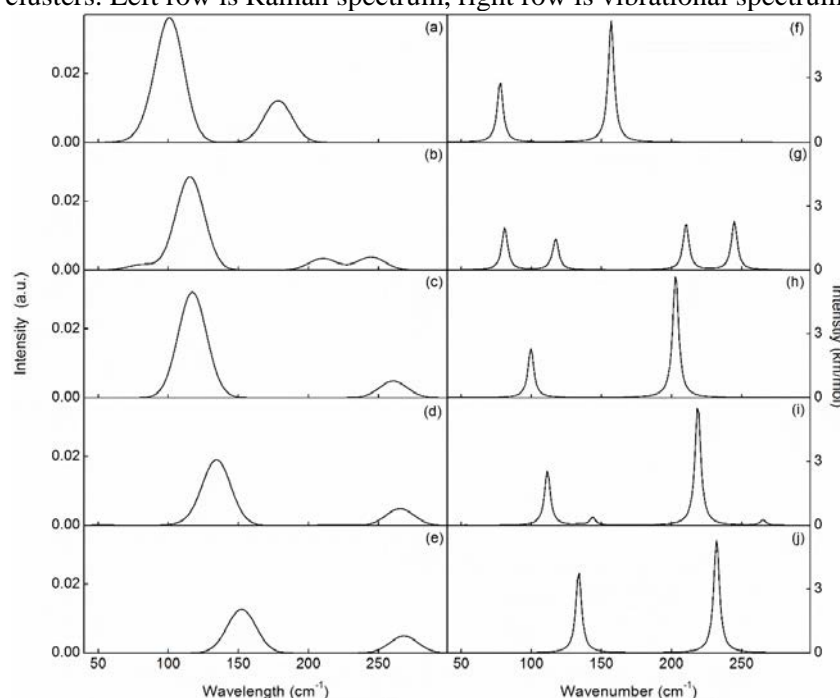


Figure 3. Raman and vibrational spectra of Ag_4 (a, f), Ag_3Cu_1 (b, g), Ag_2Cu_2 (c, h), Ag_1Cu_3 (d, i) and Cu_4 (e, j) clusters. Left row is Raman spectrum, right row is vibrational spectrum.

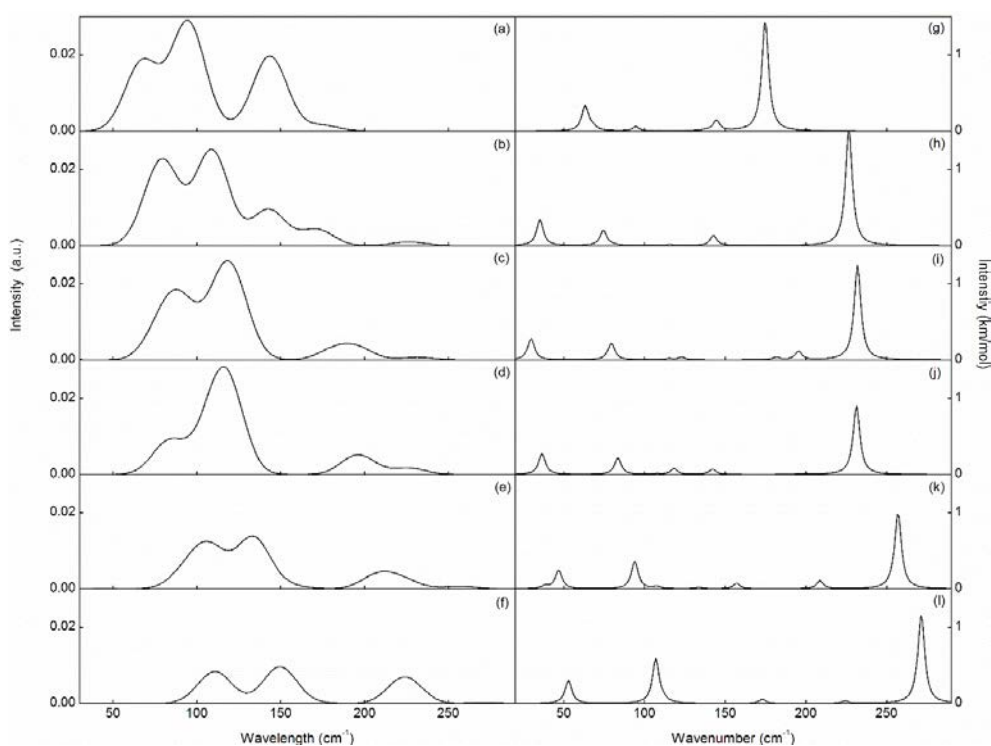


Figure 4. Raman and vibrational spectra of pure Ag_5 (a, g), Ag_4Cu_1 (b, h), Ag_3Cu_2 (c, i), Ag_2Cu_3 (d, j), Ag_1Cu_4 (e, k) and Cu_5 (f, l) clusters. Left row is Raman spectrum, right row is vibrational spectrum.

Figure 5 shows the Raman and vibrational spectra of 6-atom silver-copper nanoclusters. Their Raman and vibrational spectra are complex and have many peaks. For the strongest peaks of their Raman spectra, the wavelengths of five silver-copper clusters are larger than Ag_6 and are smaller than Cu_6 , their intensities are weaker than Ag_6 and are stronger than Cu_6 (Figure 5a-g). For the strongest peaks of Raman spectra of five silver-copper nanoclusters, the wavelengths and intensities enlarge with the amount of copper atom increasing (Figure 5b-f). For the strongest peaks of their vibrational spectra, the wavenumbers of five silver-copper clusters are bigger than Ag_6 and are smaller than Cu_6 , their intensities (except Ag_3Cu_3) are weaker than Ag_6 and Cu_6 , the intensity of Ag_3Cu_3 is stronger than Ag_6 and Cu_6 (Figure 5h-n). In the strongest peak of vibrational spectra of five silver-copper nanoclusters, Ag_1Cu_5 has the largest wavenumber, Ag_5Cu_1 has the smallest wavenumber, the wavenumber of Ag_4Cu_2 is slightly less than Ag_2Cu_4 and is slightly bigger than Ag_3Cu_3 , Ag_3Cu_3 has the strongest intensity, Ag_1Cu_5 has the weakest intensity, the intensity of Ag_5Cu_1 is slightly stronger than Ag_2Cu_4 but is a bit smaller than Ag_4Cu_2 (Figure 5i-m).

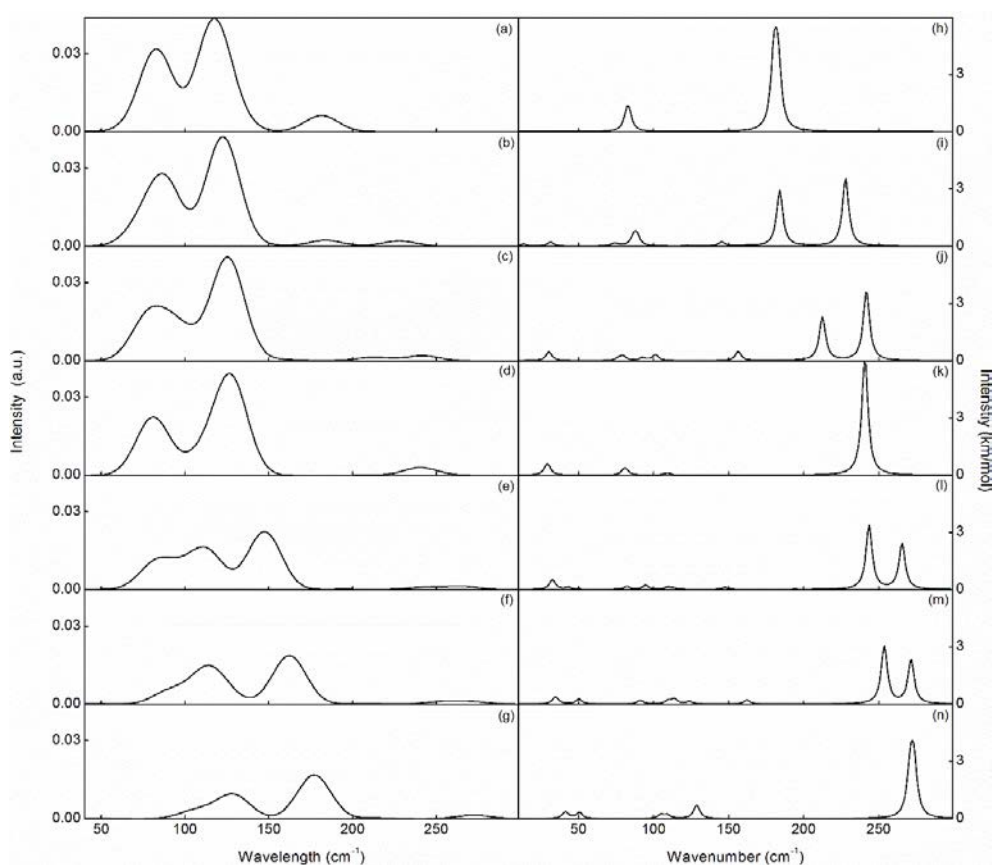


Figure 5. Raman and vibrational spectra of Ag_6 (a, h), Ag_5Cu_1 (b, i), Ag_4Cu_2 (c, j), Ag_3Cu_3 (d, k), Ag_2Cu_4 (e, l), Ag_1Cu_5 (f, m) and Cu_6 (g, n) clusters. Left row is Raman spectrum, right row is vibrational spectrum.

4. Conclusion

The electronic, Raman and vibrational properties of Ag_n , Cu_n , Ag_mCu_n ($m + n = 3-6$) clusters were calculated using DFT. As the amount of copper atom increases, E_{gap} and hardness values of the 3-5-atom silver-copper nanoclusters add, E_{gap} and hardness values of the 6-atom silver-copper nanoclusters firstly reduce, then add; electrophilicity index values of the 3-5-atom silver-copper nanoclusters decrease, electrophilicity index values of the 6-atom silver-copper nanoclusters firstly add, then reduce; electronegativity values of 3- and 6-atom silver-copper nanoclusters firstly decrease, then add, and then reduce, electronegativity values of 4- and 5-atom silver-copper increase; softness values of 3- and 6-atom silver-copper nanoclusters firstly add, then reduce, softness values of 4- and 5-atom silver-copper nanoclusters decrease. All Raman and vibrational models of silver-copper nanoclusters are related with their compositions, sizes, and geometries. As the amount of copper atom increases, the strongest Raman peak wavelengths of 3-6-atom silver-copper nanoclusters become large, and wavenumbers of the strongest vibrational peaks of 3-atom, 5-atom (except Ag_2Cu_3), and 6-atom (except Ag_3Cu_3) silver-copper almost become large. The wavenumber of the strongest vibrational peak of Ag_3Cu_1 cluster is the largest and the wavenumber of the strongest vibrational peak of Ag_2Cu_2 cluster is the smallest of 4-atom silver-copper.

Acknowledgments

This work was supported by Scientific Research Project of Ningxia High Education Institutions (Grant No. NGY2017167). The authors declare that they have no conflict of interest.

References

- [1] M. L. Brongersma, J. W. Hartman, and H. A. Atwater (2000). *Phys Rev B* **62**, 16356-16359.
- [2] M. Quinten, A. Leitner, J. R. Krenn, and F. R. Aussenegg (1998). *Opt Lett* **23**, 1331-1333.
- [3] F. Chen, and R. L. Johnston (2008). *Acta Mater* **56**, 2374-2380.
- [4] F. Chen, and R. L. Johnston (2007). *Appl Phys Lett* **90**, 153123.
- [5] L. N. Lewis (1993). *Chem Rev* **93**, 2693-2730.
- [6] H. K. Wang, F. Y. Chen, W. Y. Li, and T. Tian (2015). *J Power Sources* **287**, 150-157.
- [7] F. Chen, and R. L. Johnston (2008). *Acta Mater* **56**, 2374-2380.
- [8] F. Chen, and R. L. Johnston (2007). *Appl Phys Lett* **90**, 153123.
- [9] S. Nunez, and R. L. Johnston (2010). *J Phys Chem C* **114**, 13255-13266.
- [10] G. A. Bishea, N. Marak, and M. D. Morse (1991). *The Journal of Chemical Physics* **95**, 5618.
- [11] G. A. Bishea, C. A. Arrington, J. M. Behm, and M. D. Morse (1991). *The Journal of Chemical Physics* **95**, 8765.
- [12] M. Cazayous, C. Langlois, T. Oikawa, C. Ricolleau, and A. Sacuto (2006). *Phys Rev B* **73**, 113402.
- [13] A. M. James, G. W. Lemire, and P. R. R. Langridge-Smith (1994). *Chem. Phys. Lett.* **227**, 503-510.
- [14] P. Ranjan, S. Dhail, S. Venigalla, A. Kumar, L. Ledwani, and T. Chakraborty (2015). *Mat. Sci. Pol.* **33**, 719.
- [15] P. Ranjan, Chakraborty, T., & Kumar, A. (2018). Theoretical Analysis: Electronic, Raman, Vibrational, and Magnetic Properties of Cu_nAg (n= 1-12) Nanoalloy Clusters. In *Theoretical and Quantum Chemistry at the Dawn of the 21st Century* (pp. 25-58). Apple Academic Press.
- [16] P. Ranjan, A. Kumar, T. Chakraborty, & A. Pandey (2017). Theoretical analysis: electronic and optical properties of small Cu-Ag nano alloy clusters. *Computational Chemistry Methodology in Structural Biology and Materials Sciences*.
- [17] W. Li, and F. Chen (2013). *J Nanopart Res* **15**, 1809.
- [18] Y. Rao, Y. M. Lei, X. Y. Cui, Z. W. Liu, and F. Y. Chen (2013). *J Alloy Compd* **565**, 50-55.
- [19] W. Li, and F. Chen (2014). *Eur Phys J D* **68**, 91.
- [20] W. Li, and F. Chen (2014). *Phys B* **443**, 6-23.
- [21] W. Li, and F. Chen (2014). *J Alloy Compd* **607**, 238-244.
- [22] W. Q. Ma, and F. Y. Chen (2012). *J Alloy Compd* **541**, 79-83.
- [23] W. Li, and F. Chen (2014). *J Nanopart Res* **16**, 2498.
- [24] W. Li, and F. Chen (2014). *Chin Phys B* **23**, 117103.
- [25] W. Y. Li, S. Zhang, and L. Hai (2018). *Journal of Nanoparticle Research* **20**, 188.
- [26] J. P. Perdew, K. Burke, and M. Ernzerhof (1996). *Phys Rev Lett* **77**, 3865-3868.
- [27] B. Delley (1990). *J Chem Phys* **92**, 508-517.
- [28] B. Delley (2000). *J Chem Phys* **113**, 7756-7764.
- [29] R. G. Parr, and W. Yang (1989). Oxford, University Press: Oxford.